Formation of CH(A2Δ,B2Σ−,C2Σ+) by electron–ion recombination processes in the argon and krypton afterglow reactions of CH4

ARTICLE *in* THE JOURNAL OF CHEMICAL PHYSICS · JANUARY 1991

Impact Factor: 2.95 · DOI: 10.1063/1.460018

5 AUTHORS, INCLUDING:

Masaharu Tsuji
Kyushu University
441 PUBLICATIONS **6,231** CITATIONS

SEE PROFILE

Formation of CH(A2Δ,B2Σ−,C2Σ+) by electron–ion recombination processes in the argon and krypton afterglow reactions of CH4

Masaharu Tsuji, Kazunari Kobarai, Hiroyuki Kouno, Hiroshi Obase, and Yukio Nishimura

Citation: J. Chem. Phys. **94**, 1127 (1991); doi: 10.1063/1.460018
View online: http://dx.doi.org/10.1063/1.460018
View Table of Contents: http://jcp.aip.org/resource/1/JCPSA6/v94/i2
Published by the American Institute of Physics.

Formation of CH($A\,^2\Delta$,$B\,^2\Sigma^-$,$C\,^2\Sigma^+$) by electron–ion recombination processes in the argon and krypton afterglow reactions of CH_4

Masaharu Tsuji, Kazunari Kobarai,[a] Hiroyuki Kouno, Hiroshi Obase,[b] and Yukio Nishimura

Institute of Advanced Material Study and Department of Molecular Science and Technology, Graduate School of Engineering Sciences, Kyushu University, Kasuga-shi, Fukuoka 816, Japan

(Received 23 July 1990; accepted 3 October 1990)

The CH(A–X,B–X,C–X) emission systems have been observed from the Ar and Kr afterglow reactions of CH_4. A significant attenuation of the CH(A–X,B–X,C–X) emissions by an addition of SF_6 into the discharge flow suggested that the CH(A,B,C) radicals are excited via secondary electron–ion recombination processes. Since the CH(A–X,B–X,C–X) emissions disappeared by trapping ionic active species in the discharge flow, the responsible active species for the CH(A,B,C) production were found to be Ar^+ and/or $(Ar^+)^*$ in the Ar flow and Kr^+ and/or $(Kr^+)^*$ in the Kr flow. The contribution of Ar^+ and Kr^+ was examined in the He afterglow, where Ar^+ or Kr^+ and slow electrons were simultaneously produced by the He(2^3S)/Ar,Kr Penning ionization. Although intense CH(A–X,B–X,C–X) emissions were observed from Ar^+/CH_4 where CH_n^+ ($n = 2$–4) were formed, they were absent from Kr^+/CH_4 where only CH_4^+ was produced. It was, therefore, concluded that CH_2^+ and/or CH_3^+ are important precursor ions for the CH(A,B,C) production. The intensity distribution of CH(A,B,C) and the CH(A,B) rovibrational distributions obtained in the Ar afterglow agreed with those through Ar^+/CH_4, indicating that Ar^+/CH_4 plays a significant role for the production of precursor ions in the Ar afterglow or $(Ar^+)^*/CH_4$ provides the same precursor ions. Since the relative intensity of CH(A,B) and the rovibrational distributions of CH(A) in the Kr afterglow were different from those in the Ar afterglow, different electron–ion recombination processes dominantly take part in the CH(A,B) production.

I. INTRODUCTION

Prince *et al.*,[1] and Suzuki and Kuchitsu[2] observed the CH($A\,^2\Delta$–$X\,^2\Pi_r$) emission system in the Ar afterglow reaction of CH_4. Both groups used a microwave discharge for the generation of Ar active species. Although the former assumed the excitation source to be $Ar(^3P_{2,0})$, the latter pointed out that the formation of CH(A) from the $Ar(^3P_{2,0})/CH_4$ reaction is energetically inaccessible:

$$Ar(^3P_2) + CH_4 \rightarrow CH(A) + H_2(X\,^1\Sigma_g^+) + H(n=1) + Ar - 0.40\ \text{eV}, \quad (1a)$$

$$Ar(^3P_0) + CH_4 \rightarrow CH(A) + H_2(X\,^1\Sigma_g^+) + H(n=1) + Ar - 0.20\ \text{eV}. \quad (1b)$$

Suzuki and Kuchitsu[2] found that ionic species were responsible for the CH(A) production because the emission intensity decreased rapidly by an application of a negative potential to an ion-collector grid placed between the discharge section and the reaction zone. The responsible active species were predicted to be metastable ions $(Ar^+)^*$, because the Ar pressure dependence of CH(A–X) was similar to that of Cl* from the $(Ar^+)^*/HCl$ reaction[3] and Kr* from the $(Ar^+)^*/Kr$ reaction.[4] Suzuki and Kuchitsu[2] estimated the vibrational and rotational distributions of CH(A) to be $N_0(T_0)$: $N_1(T_1)$: $N_2(T_2) = 100(T_0 = 3000 \pm 1500$ K): $56(T_1 = 1700 \pm 500$ K): $10(T_2 = 1000$ K) from a spectral simulation. In addition to CH(A–X), the CH($B\,^2\Sigma^-$–$X\,^2\Pi_r$) emission system was found in the Ar afterglow reaction of CH_4 by Suzuki and Kuchitsu.[2] However, the intensity ratio of CH(B–X)/CH(A–X) and the rovibrational distribution of CH(B) have not been determined. Although electron–ion recombination processes often take part in the formation of neutral excited species in the flowing afterglow (FA), their contribution has not been examined in the previous FA experiments for the CH(A,B) production from the Ar afterglow reaction of CH_4.[1,2]

In the present study, the CH(A–X,B–X,C–X) emission systems are observed from reactions of ionic active species with CH_4 in the Ar and Kr afterglows. The disappearance of CH(A–X,B–X,C–X) by an addition of SF_6 into the discharge flow indicates that all of CH(A,B,C) are formed via secondary electron–ion recombination processes, where precursor ions are produced by the reactions with rare gas ions in the ground states (Ar^+,Kr^+) and/or in the metastable states [$(Ar^+)^*$,$(Kr^+)^*$]. In order to determine the contribution of Ar^+ and Kr^+ to the formation of precursor CH_n^+ ions, electron–ion recombination reactions are studied in the He discharge flow, in which precursor CH_n^+ ($n = 2$–4) ions are produced by the charge-transfer reactions of Ar^+ or Kr^+ with CH_4, and electrons are generated by the He (2^3S) Penning ionization of Ar or Kr. The intensity distribution of CH(A,B,C) and the rovibrational distributions of CH(A,B) are determined.

[a] Present address: Nakatsu Technical High School, Nakatsu, Oita 871, Japan.

[b] Present address: Department of Industrial Chemistry, Faculty of Engineering, Towa University, Chikushigaoka, Minami-ku, Fukuoka 815, Japan.

 0021-9606/91/021127-07$03.00

II. EXPERIMENTAL

The FA apparatus used in this study has been described in detail.[5] Rare gas active species were generated by a microwave discharge of high purity rare gas in a discharge flow operated at 0.06–0.6 Torr (1 Torr = 133.3 Pa) for Ar and 0.04–0.07 Torr for Kr. The sample CH_4 gas was admixed with the discharge flow about 10 cm downstream from the center of the discharge. The partial pressure of CH_4 in the reaction zone was 2–20 mTorr. The active species involved in the Ar and Kr discharge flows were examined by observing optical emissions resulting from suitable reference reactions for metastable atoms and ions.[6,7] It was found that $Ar(^3P_{2,0})$, Ar^+, and $(Ar^+)^*$ were involved in the Ar discharge flow, whereas $Kr(^3P_2)$, Kr^+, and $(Kr^+)^*$ were present in the Kr flow under operating conditions. Metastable atoms were dominant active species at low rare gas pressures below 0.15 Torr for Ar and 0.05 Torr for Kr, while ionic species became significant at higher pressures. The contribution of ionic active species to the observed emissions was examined by using an ion-collector grid placed between the discharge section and the reaction zone. The efficiency of ion collection was found to be $>98\%$ in all cases.

In addition to the conventional FA experiment described above, a new type of FA experiment was carried out for an optical spectroscopic study on electron–ion recombination reactions. The schematic diagram of the apparatus is shown in Fig. 1. Metastable $He(2^3S)$ atoms and He^+ and He_2^+ ions were generated by a microwave discharge of high purity He operated at 0.6–1.8 Torr. After trapping the ionic active species by using a pair of grids, the $He(2^3S)$ atoms flowed downstream past the first gas inlet from which a small amount of the Ar, Kr, or Xe gas was introduced. Ar^+, Kr^+, or Xe^+ ions in the ground electronic states, $^2P_{1/2}$ and $^2P_{3/2}$, and electrons were simultaneously produced by Penning ionization:

$$He(2^3S) + Ar \rightarrow Ar^+(^2P_{3/2,1/2}) + He + e^-, \quad (2)$$

$$He(2^3S) + Kr \rightarrow Kr^+(^2P_{3/2,1/2}) + He + e^-, \quad (3)$$

$$He(2^3S) + Xe \rightarrow Xe^+(^2P_{3/2,1/2}) + He + e^-. \quad (4)$$

The rate constants for processes (2)–(4) have been measured as (7–9), (10–14), and (12–18) $\times 10^{-11}$ $cm^3\ s^{-1}$, respectively.[8] The population ratios of $^2P_{3/2}/^2P_{1/2}$ in Kr^+ and Xe^+ were estimated by observing $KrF(B–X,D–X)$ and $XeF(B–X,D–X)$ excimer emissions produced from the following spin–orbit state selective reactions:[9]

$$Kr^+(^2P_{3/2}) + SF_6^- \rightarrow KrF(B) + SF_5, \quad (5a)$$

$$Kr^+(^2P_{1/2}) + SF_6^- \rightarrow KrF(D) + SF_5, \quad (5b)$$

$$Xe^+(^2P_{3/2}) + SF_6^- \rightarrow XeF(B) + SF_5, \quad (6a)$$

$$Xe^+(^2P_{1/2}) + SF_6^- \rightarrow XeF(D) + SF_5, \quad (6b)$$

where SF_6^- was formed by an attachment of Penning electrons to SF_6:

$$SF_6 + e^- \rightarrow SF_6^-. \quad (7)$$

It was found that most of the Kr^+ and Xe^+ ions in the reaction zone was in the lower $^2P_{3/2}$ spin–orbit state. Such a technique could not be applied to the estimation of the $^2P_{3/2}/^2P_{1/2}$ ratio in Ar^+, because $ArF(B–X,D–X)$ emissions were heavily overlapped with each other.[10,11] Since the energy interval between the two spin–orbit states in Ar^+ (0.18 eV) is smaller than those in Kr^+ (0.67 eV) and Xe^+ (1.31 eV), the collisional relaxation from the upper $^2P_{1/2}$ state to the lower $^2P_{3/2}$ state in the He flow is expected to be much faster for Ar^+. It is likely, therefore, most of Ar^+ is also populated in the lower $^2P_{3/2}$ state. The sample CH_4 gas was introduced into the discharge flow though the second inlet placed about 10 cm downstream from the first gas inlet. The partial pressure in the reaction zone was 10–50 mTorr for Ar, Kr, or Xe and 5–20 mTorr for CH_4.

A conical reaction flame observed around the CH_4 gas inlet was dispersed with a Jarrell Ash 1.0 m monochromator fitted with a 300 nm blazed grating and equipped with a cooled Hamamatsu Photonics R376 photomultiplier. The monochromator and the optical detection system were calibrated by using standard lamps.

III. RESULTS AND DISCUSSION

A. Excitation processes in the Ar and Kr afterglows

Figure 2 shows a typical emission spectrum obtained from the Ar afterglow reaction of CH_4. Besides the $CH(A\,^2\Delta–X\,^2\Pi_r, B\,^2\Sigma^- –X\,^2\Pi_r)$ emission systems reported previously,[1,2] a weak $CH(C\,^2\Sigma^+ –X\,^2\Pi_r)$ emission system is identified around 315 nm. It was found that Ar^+ and/or $(Ar^+)^*$ ions participated in the formation of $CH(C)$ as well as $CH(A,B)$, because the $CH(C–X)$ band disappeared by ion trapping. The recombination energy of $Ar^+(^2P_{3/2})$ is 15.76 eV, and the available energies of $(Ar^+)^*$ are 16.41–20.27 eV for the $(Ar^+)^* \rightarrow Ar^+$ excitation transfer and 17.87–22.19 eV for the $(Ar^+)^* \rightarrow Ar^*$ charge transfer.[6] Ta-

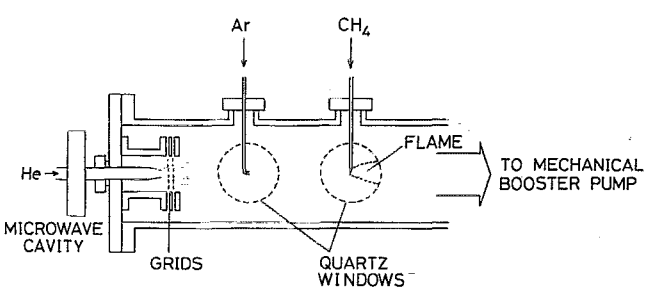

FIG. 1. The flowing afterglow apparatus for studying electron–ion recombination reactions.

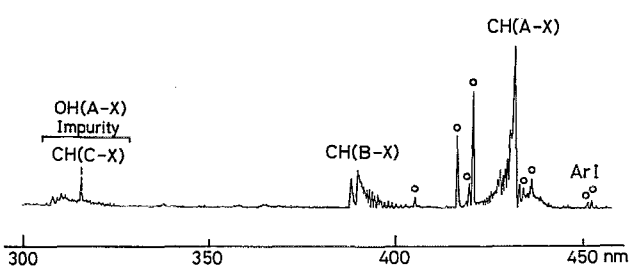

FIG. 2. Emission spectrum obtained from the Ar afterglow reaction of CH_4. The lines marked O are stray ArI lines. The optical resolution is 3.8 Å (FWHM).

ble I summarizes the calculated minimum energies for the formation of $CH(A,B,C)$ and CH_n^+ $(n=1$–$4)$ from CH_4. On the basis of energetics, the $(Ar^+)^*$ ions have sufficient energy to produce $CH(A,B,C)$. However, $CH(A,B,C)$ cannot be produced by the Ar^+/CH_4 charge-transfer reaction. In our recent FA studies on the isovalent SiH_4 and GeH_4 molecules,[7,14–16] we have found that both primary reactions of rare gas active species with the sample gases and secondary reactions involving ion–electron recombination take part in the production of neutral excited species. Therefore, the following primary and secondary processes are possible for the $CH(A,B,C)$ production:

primary processes

$$(Ar^+)^* + CH_4 \rightarrow CH(A,B,C) + H_2 + H + Ar^+, \quad (8a)$$

$$\rightarrow CH(A,B,C) + 3H + Ar^+, \quad (8b)$$

secondary processes via electron–ion recombination

$$(Ar^+)^* + CH_4 \rightarrow CH_n^+ (n=2\text{–}4) + (H_2 \text{ and/or } H) + Ar^+ + e^-, \quad (9a)$$

$$\rightarrow CH_n^+ (n=2\text{–}4) + (H_2 \text{ and/or } H) + Ar^*, \quad (9b)$$

$$\rightarrow CH^+ + H_2 + H + Ar^+ + e^-, \quad (9c)$$

$$\rightarrow CH^+ + H_2 + H + Ar^*, \quad (9d)$$

$$Ar^+(^2P_{3/2}) + CH_4 \rightarrow CH_4^+ + Ar, \quad (10a)$$

$$\rightarrow CH_2^+ + H + Ar, \quad (10b)$$

$$\rightarrow CH_2^+ + H_2 + Ar, \quad (10c)$$

$k_{10a} = 0.82, k_{10b} = 6.6$, and $k_{10c} = 0.82$ in 10^{-10} $cm^3 s^{-1}$ units,[17]

$$e^- + CH_n^+ (n=2\text{–}4) \rightarrow CH(A,B,C) + (H_2 \text{ and/or } H), \quad (11a)$$

$$e^- + CH^+ + Ar \rightarrow CH(A,B,C) + Ar. \quad (11b)$$

If $CH(A,B,C)$ are produced through the secondary processes, Ar^+ as well as $(Ar^+)^*$ can take part in the reaction. Ar^+ ions in process (10) are produced in the Ar discharge and through processes (8), (9a), and (9c). The effect of electron–ion recombination processes has been examined by adding SF_6 into the reaction zone. SF_6 not only attaches thermal electrons very rapidly ($k = 2.2\times10^{-7}$ $cm^3 s^{-1}$)[18] but also quenches $(Ar^+)^*$. Therefore, the reduction of $[(Ar^+)^*]$ by the addition of SF_6 should be corrected. In the present study, the decrease in $[(Ar^+)^*]$ by the SF_6 addition was corrected by observing Kr* lines resulting from the $(Ar^+)^*/Kr$ reaction:[4]

$$(Ar^+)^* + Kr \rightarrow Kr^* + Ar^+. \quad (12)$$

Figure 3 shows the dependence of $CH(A$–$X)$ and Kr* emission intensities on the added SF_6 concentration at a constant CH_4 concentration. The Kr* line decreases with increasing the $[SF_6]/[CH_4]$ ratio due to quenching of $(Ar^+)^*$ by SF_6. It should be noted that the $CH(A$–$X)$ emission decreases more rapidly with $[SF_6]/[CH_4]$ and almost disappears at a high $[SF_6]/[CH_4]$ ratio of ~ 2. A similar tendency was found for $CH(B$–$X)$ and $CH(C$–$X)$. These results lead us to conclude that all of the $CH(A,B,C)$ states are excited via electron–ion recombination processes (11).

When emission spectra of CH_4 in the Kr afterglow were observed at low Kr pressures below ~ 50 mTorr, where only $Kr(^3P_2)$ was involved in the discharge flow, no emission was detected. At high Kr pressures above ~ 60 mTorr, where $Kr(^3P_2)$, Kr^+, and $(Kr^+)^*$ were present, the $CH(A$–X, B–$X)$ emission systems were found as shown in Fig. 4. Outstanding features of the CH emission in the Kr afterglow in comparison with that in the Ar afterglow are that the B–X system becomes weak and the C–X system cannot be detected. When the ionic active species were trapped by using the ion-collector grid, the $CH(A$–X, B–$X)$ emissions disappeared completely. This suggests that Kr^+ and/or $(Kr^+)^*$ are responsible for the $CH(A,B)$ production. The recombi-

TABLE I. Calculated minimum energies for the production of $CH(A,B,C)$ and CH_n^+ $(n=1$–$4)$ from CH_4.[a]

Products	ΔH_0° (eV)
$CH_4 \rightarrow CH(A\,^2\Delta) + H_2(X\,^1\Sigma_g^+) + H(n=1)$	12.0
$\rightarrow CH(A\,^2\Delta) + 3H(n=1)$	16.4
$\rightarrow CH(B\,^2\Sigma^-) + H_2(X\,^1\Sigma_g^+) + H(n=1)$	12.3
$\rightarrow CH(B\,^2\Sigma^-) + 3H(n=1)$	16.7
$\rightarrow CH(C\,^2\Sigma^+) + H_2(X\,^1\Sigma_g^+) + H(n=1)$	13.1
$\rightarrow CH(C\,^2\Sigma^+) + 3H(n=1)$	17.5
$\rightarrow CH_4^+ + e^-$	12.6
$\rightarrow CH_3^+ + H(n=1) + e^-$	13.6
$\rightarrow CH_2^+ + H_2(X\,^1\Sigma_g^+) + e^-$	14.5
$\rightarrow CH_2^+ + 2H(n=1) + e^-$	19.0
$\rightarrow CH^+(X\,^1\Sigma^+) + H_2(X\,^1\Sigma_g^+) + H(n=1) + e^-$	19.0

[a]The ΔH_0° values are estimated from thermochemical and spectroscopic data in Refs. 12 and 13.

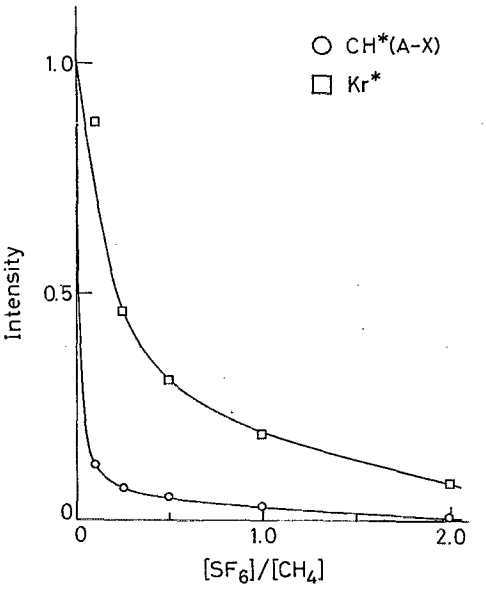

FIG. 3. The dependence of $CH(A$–$X)$ and Kr* emission intensities on the $[SF_6]/[CH_4]$ ratio.

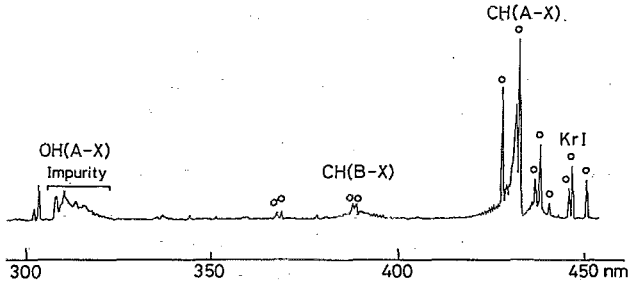

FIG. 4. Emission spectrum obtained from the Kr afterglow reaction of CH_4. The lines marked ○ are stray KrI lines. The optical resolution is 4.7 Å (FWHM).

nation energy of $Kr^+(^2P_{3/2})$ is 14.00 eV, whereas the available energies of $(Kr^+)^*$ are 14.90–16.32 for the $(Kr^+)^* \rightarrow Kr^+$ excitation transfer and 15.90–18.32 eV for the $(Kr^+)^* \rightarrow Kr^*$ charge transfer.[7] By addition of a small amount of SF_6 into the Kr discharge flow, the CH(*A–X, B–X*) emissions disappeared as in the case of Ar discharge flow. On the basis of these findings and the energetics, all of CH(*A,B*) are produced through the Kr^+/CH_4 and/or $(Kr^+)^*/CH_4$ reactions followed by electron–ion recombination processes:

$$Kr^+(^2P_{3/2}) + CH_4 \rightarrow CH_4^+ + Kr, \quad (13)$$

$$k_{13} = 1.0\times10^{-9}\ cm^3\ s^{-1}\ (Ref.\ 19),$$

$$(Kr^+)^* + CH_4 \rightarrow CH_n^+\ (n = 2\text{–}4) + (H_2\ and/or\ H) + Kr^+ + e^-, \quad (14a)$$

$$\rightarrow CH_n^+\ (n = 2\text{–}4) + (H_2\ and/or\ H) + Kr^*, \quad (14b)$$

$$e^- + CH_n^+\ (n = 2\text{–}4) \rightarrow CH(A,B) + (H_2\ and/or\ H). \quad (11a')$$

B. Excitation processes in the He afterglow

In the Ar and Kr afterglow reactions of CH_4, there are two possible ionic sources for the production of precursor ions of CH(*A,B*): ground state ions (Ar^+ and Kr^+) and metastable ions [$(Ar^+)^*$ and $(Kr^+)^*$]. It was difficult to determine their relative contributions, because selective formation of one ionic species was not possible. In order to determine whether Ar^+ and Kr^+ participate in the reactions, emission spectra resulting from the Ar^+/CH_4 and Kr^+/CH_4 reactions followed by electron–ion recombination processes were observed by using the He(2^3S) Penning ionization of Ar and Kr. The Xe^+/CH_4 reaction was also used for the production of precursor ions. The coexistence of Ar^+, Kr^+, or Xe^+ and electrons in the reaction zone was confirmed by observing ArF(*B–X*), KrF(*B–X*), and XeF(*B–X*) resulting from the following ion-recombination reactions:[9,10]

$$Ar^+(^2P_{3/2}) + SF_6^- \rightarrow ArF(B) + SF_5, \quad (15)$$

$$Kr^+(^2P_{3/2}) + SF_6^- \rightarrow KrF(B) + SF_5, \quad (5a)$$

$$Xe^+(^2P_{3/2}) + SF_6^- \rightarrow XeF(B) + SF_5. \quad (6a)$$

When the $Ar^+(^2P_{3/2})/CH_4$ reaction was used for the production of precursor ions, strong CH(*A–X,B–X,C–X*) emissions were observed as shown in Fig. 5. On the other hand, no emission could be found, when precursor ions were formed by the $Kr^+(^2P_{3/2})/CH_4$ and $Xe^+(^2P_{3/2})/CH_4$ reactions. These results show that precursor ions are produced from the $Ar^+(^2P_{3/2})/CH_4$ reaction, but the $Kr^+(^2P_{3/2})/CH_4$ and $Xe^+(^2P_{3/2})/CH_4$ reactions do not provide precursor ions. Thus, the $Ar^+(^2P_{3/2})/CH_4$ reaction must take part in the CH(*A,B,C*) formation in the Ar afterglow, while the $Kr^+(^2P_{3/2})/CH_4$ reaction does not contribute to the CH(*A,B*) formation in the Kr afterglow. The appearance of CH(*A–X,B–X*) in the Kr afterglow leads us to conclude that all CH(*A–X,B–X*) emissions result from the $(Kr^+)^*/CH_4$ reaction followed by electron–ion recombination processes. No direct evidence of the contribution of the $(Ar^+)^*/CH_4$ reaction to the CH(*A,B,C*) production in the Ar afterglow was obtained. However, it may be reasonable to assume that the $(Ar^+)^*/CH_4$ reaction also participates in the CH(*A,B,C*) production, because the available energies of $(Ar^+)^*$ are higher than those of $(Kr^+)^*$.

According to mass spectroscopic data, the Ar^+/CH_4 reaction at thermal energy provides CH_4^+, CH_3^+, and CH_2^+ ions with branching fractions of 0.10: 0.80: 0.10, respectively,[17] whereas only parent CH_4^+ ions are formed by the $Kr^+(^2P_{3/2})/CH_4$ and $Xe^+(^2P_{3/2})/CH_4$ reactions.[19] From the present results, dominant precursor ions for the CH(*A,B,C*) production in the Ar afterglow reaction of CH_4 are not CH_4^+ but CH_3^+ and/or CH_2^+.

Suzuki and Kuchitsu[2] concluded that $(Ar^+)^*$ is responsible for the CH(*A*) production in the Ar afterglow reaction of CH_4, because the Ar pressure dependence of CH(*A–X*) was similar to that of Cl* from $(Ar^+)^*/HCl$[3] and Kr* from $(Ar^+)^*/Kr$[4] in the Ar afterglow. We compared the Ar pressure dependence of CH(*A–X*) with that of Kr* from $(Ar^+)^*/Kr$ and $OCS^+(\tilde{A}\text{–}\tilde{X})$ from Ar^+/OCS.[20,21] The Ar pressure dependence of CH(*A–X*) was similar to that of Kr* in agreement with the result of Suzuki and Kuchitsu.[2] However, a significant discrepancy is found between the Ar pressure dependence of CH(*A–X*) and $OCS^+(\tilde{A}\text{–}\tilde{X})$, though Ar^+ must contribute to the formation of CH(*A*). This discrepancy is discussed below by a kinetic analysis of the reaction processes.

On the basis of the present results, CH(*A*) probably results from secondary processes (9)–(11). Assuming a steady state condition for precursor CH_n^+ ($n = 1$–4) ions, the production rate of CH(*A*) is given by

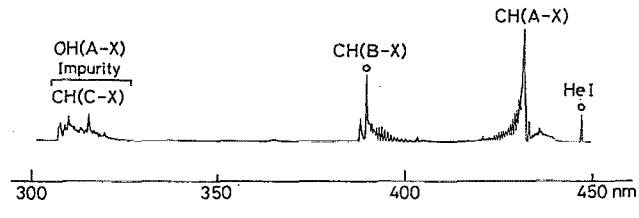

FIG. 5. CH(*A–X,B–X,C–X*) emissions obtained through electron–ion recombination reactions in the He afterglow, where precursor ions are produced via $Ar^+(^2P_{3/2})/CH_4$ reaction. The optical resolution is 2.9 Å (FWHM).

$$\frac{d[\mathrm{CH}(A)]}{dt} = (k_{9a} + k_{9b} + k_{9c} + k_{9d})[(\mathrm{Ar}^+)^*][\mathrm{CH_4}] + (k_{10b} + k_{10c})[\mathrm{Ar}^+][\mathrm{CH_4}]. \quad (17)$$

On the other hand, if a steady state condition is assumed for thermal electrons produced from reactions (9a) and (9c), the production rate of $\mathrm{CH}(A)$ is expressed by

$$\frac{d[\mathrm{CH}(A)]}{dt} = (k_{9a} + k_{9c})[(\mathrm{Ar}^+)^*][\mathrm{CH_4}]. \quad (18)$$

Although the latter assumption explains the observed Ar pressure dependence of $\mathrm{CH}(A,B)$, the former assumption does not reproduce it without assuming $(k_{9a} + k_{9b} + k_{9c} + k_{9d})[(\mathrm{Ar}^+)^*] \gg (k_{10b} + k_{10c})[\mathrm{Ar}^+]$. It seems unlikely that this relation holds under the operating conditions, because Ar^+ is an effective source of the production of precursor ions based upon the present study on the $\mathrm{Ar}^+/\mathrm{CH_4}$ reaction in the He afterglow. Consequently, a strong correlation of $\mathrm{CH}(A$–$X)$ with $(\mathrm{Ar}^+)^*$ in the Ar pressure dependence is probably attributable to the fact that the rate determining step for the $\mathrm{CH}(A)$ production is the formation of thermal electrons from processes (9a) and (9c).

C. Rovibrational distributions of CH(*A,B*)

Relative vibrational and rotational distributions of $\mathrm{CH}(A,B)$ produced by electron–ion recombination processes were determined by a computer simulation of $\mathrm{CH}(A$–X,B–$X)$. The band intensity (photons s^{-1}) of a transition from a (v',J') level to a (v'',J'') level is expressed as

$$I_{v'J'v''J''} \propto N_{v'J'} R_e^2(\bar{r}_{v'v''}) q_{v'v''} \nu^3_{v'J'v''J''} S_{J'J''}/(2J'+1), \quad (19)$$

where $N_{v'J'}$ is the rotational population in a given vibrational level, $R_e(\bar{r}_{v'v''})$ the electronic transition moment, $q_{v'v''}$ the Franck–Condon factor, $\nu_{v'J'v''J''}$ the transition frequency, and $S_{J'J''}$ is the rotational line strength. The electronic transition moment for $\mathrm{CH}(A$–$X)$ was assumed to be constant. The following RKR Franck–Condon factors calculated by using molecular constants tabulated in Ref. 13 were employed for the simulation of the $\Delta v = 0$ sequence of $\mathrm{CH}(A$–$X)$: $q_{0,0} = 0.9907$, $q_{1,1} = 0.9794$, and $q_{2,2} = 0.9793$. The rotational line strength $S_{J'J''}$ was deduced from the formula given by Kovács.[22] A Gaussian slit function was convoluted into rotational lines to calculate the spectral envelope. Figures. 6–8 show the observed and best fit spectra of the $\Delta v = 0$ sequence of $\mathrm{CH}(A$–$X)$ and the (0,0) band of $\mathrm{CH}(B$–$X)$ obtained assuming single or double Boltzmann rotational distributions for each v' level.

The vibrational and rotational distributions thus obtained are given in Table II together with the previous data by Suzuki and Kuchitsu[2] on $\mathrm{CH}(A)$ in the Ar afterglow reaction of $\mathrm{CH_4}$. According to our recent optical spectroscopic study on the formation of $\mathrm{CH}(A,B)$ from the $\mathrm{He}(2^3S)/\mathrm{CH_4}$ reaction,[23] the vibrational and rotational re-

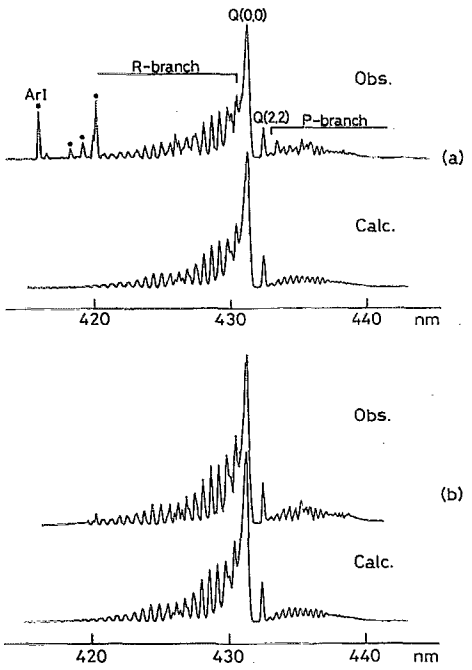

FIG. 6. The observed and calculated spectra of $\mathrm{CH}(A\,^2\Delta$–$X\,^2\Pi_r)$ obtained from (a) electron–ion recombination reactions in the Ar afterglow and (b) $e^-/\mathrm{CH_2^+}$ and/or $e^-/\mathrm{CH_3^+}$ reactions in the He afterglow. The optical resolution is 1.8 Å (FWHM) for both (a) and (b).

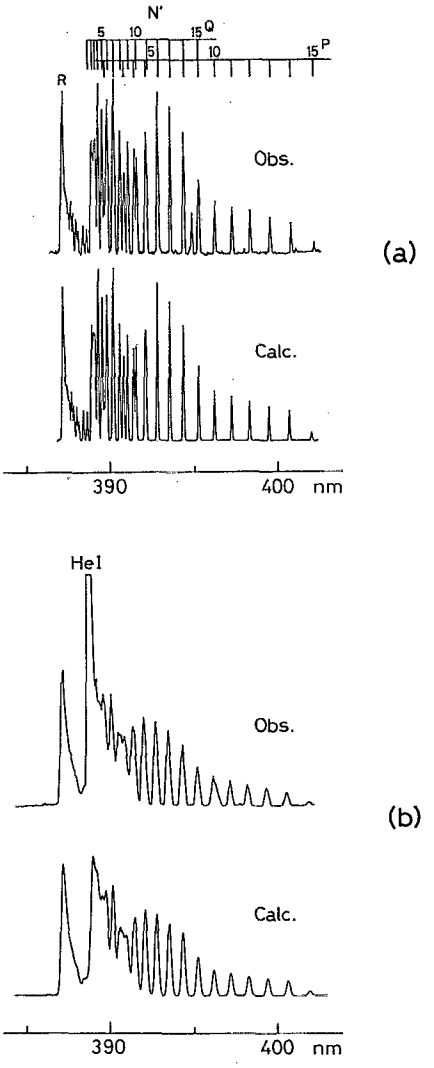

FIG. 7. The observed and calculated spectra of $\mathrm{CH}(B\,^2\Sigma^-$–$X\,^2\Pi_r)$ obtained from (a) electron–ion recombination reactions in the Ar afterglow and (b) $e^-/\mathrm{CH_2^+}$ and/or $e^-/\mathrm{CH_3^+}$ reactions in the He afterglow. The optical resolution is 0.8 Å (FWHM) for (a) and 2.5 Å for (b).

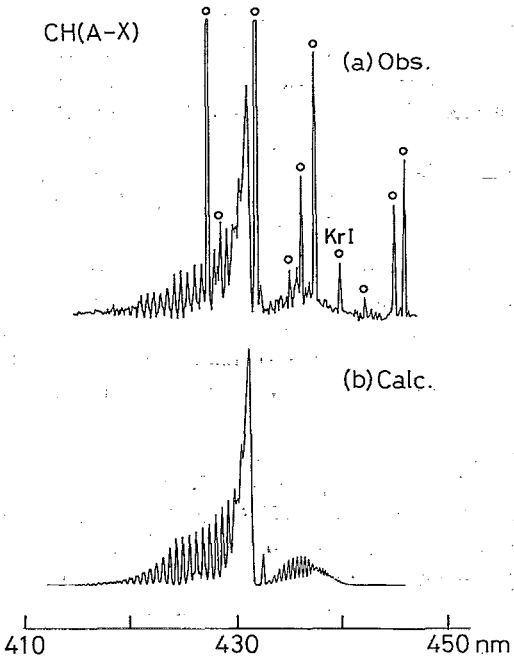

FIG. 8. The observed and calculated spectra of CH($A\,^2\Delta$–$X\,^2\Pi_r$) obtained from (a) electron–ion recombination reactions in the Kr afterglow. The optical resolution is 1.8 Å (FWHM).

laxation of CH(A,B) by collisions with the buffer He gas is insignificant in the FA experiment during radiative lifetimes of ~0.53 and ~0.35 μs, respectively.[24] Therefore, the observed rovibrational distributions of CH(A,B) are expected to reflect nascent populations. The rovibrational distribution of CH(A) in the Ar afterglow obtained in the present study is close to that reported by Suzuki and Kuchitsu.[2] It should be noted that rovibrational distributions of CH(A,B) in the Ar afterglow reaction of CH_4 are identical with those produced through the Ar^+/CH_4 reaction in the He afterglow. A similar resemblance was found for the relative intensities of CH(A,B,C). The CH(A): CH(B): CH(C) ratios were measured to be 100:23:1, respectively, for both cases. On the basis of these findings, it is reasonable to assume that the Ar^+/CH_4 reaction plays a significant role for the CH(A,B,C) production in the Ar afterglow or the $(Ar^+)^*/CH_4$ reaction gives the same precursor ions: e.g., CH_2^+ and/or CH_3^+. The rotational distribution of CH(A:$v'=0$) produced in the Ar afterglow and through the Ar^+/CH_4 reaction can be expressed by double Boltzmann distributions. This probably implies that two processes are involved in the formation of CH(A). The rovibrational distribution of CH(A) in the Kr afterglow is different from that in the Ar afterglow; CH(A) in the Kr afterglow is less vibrationally excited but more rotationally excited than that in the Ar afterglow. A significant discrepancy is also found for the relative intensities of CH(A,B,C). The CH(A): CH(B): CH(C) ratios were measured as 100:10:0, respectively. Based upon these facts, dominant electron–ion recombination processes leading to CH(A,B) in the Kr afterglow are different from those in the Ar afterglow.

The average vibrational and rotational energies of CH(A,B) were evaluated from the rovibrational distributions by using the relations:

$$\langle E_{v'} \rangle = \sum_{v'} N_{v'} E_{v'} / \sum_{v'} N_{v'}, \tag{20}$$

$$\langle E_{J'} \rangle = \sum_{v'} \sum_{J'} N_{v'J'} E_{J'} / \sum_{v'} \sum_{J'} N_{v'J'}, \tag{21}$$

where $E_{v'}$ and $E_{J'}$ are the vibrational and rotational energies, respectively. The $\langle E_{v'} \rangle$ and $\langle E_{J'} \rangle$ values are summarized in Table III. The $\langle E_{J'} \rangle$ values are larger than the $\langle E_{v'} \rangle$ values in all cases. The energetics of possible electron-ion recombination processes through the Ar^+/CH_4 reaction in the He afterglow are as follows:

$$e^- + CH_3^+ \rightarrow CH(A{:}v'=0) + H_2(X\,^1\Sigma_g^+) + 2.3 \text{ eV}, \tag{22a}$$

$$e^- + CH_3^+ \rightarrow CH(B{:}v'=0) + H_2(X\,^1\Sigma_g^+) + 2.0 \text{ eV}, \tag{22b}$$

TABLE II. The rovibrational distributions of CH($A\,^2\Delta$,$B\,^2\Sigma^-$) produced from electron-ion recombination processes in the flowing afterglow.

	Ar^+,$(Ar^+)^*/CH_4$[a] CH($A\,^2\Delta$)				Ar^+/CH_4[b] CH($A\,^2\Delta$)		$(Kr^+)^*/CH_4$[c] CH($A\,^2\Delta$)	
	This work		Suzuki and Kuchitsu[d]		This work		This work	
	$N_{v'}$	T_r (K)	$N_{v'}$	T_r (K)	$N_{v'}$	T_r (K)	$N_{v'}$	T_r (K)
$v'=0$	72 ± 8 28 ± 8	3200 ± 700 500 ± 100	100	3000 ± 1500	72 ± 8 28 ± 8	3200 ± 700 500 ± 100	100	2900 ± 300
$v'=1$	40 ± 5	1700 ± 400	56	1700 ± 400	40 ± 5	1700 ± 400	25 ± 5	2100 ± 300
$v'=2$	10 ± 1	1200 ± 300	10	1000	10 ± 1	1200 ± 300	4 ± 1	1500 ± 900

	CH($B\,^2\Sigma^-$)		CH($B\,^2\Sigma^-$)	
	This work		This work	
	$N_{v'}$	T_r (K)	$N_{v'}$	T_r (K)
$v'=0$	65 ± 4 35 ± 4	3200 ± 1100 650 ± 50	65 ± 4 35 ± 4	3800 ± 1100 650 ± 50

[a] Measured in the Ar afterglow.
[b] Measured in the He afterglow (see the text).
[c] Measured in the Kr afterglow.
[d] Reference 2.

TABLE III. Average vibrational and rotational energies deposited into the CH(A,B).

Energies (eV)	Processes $Ar^+,(Ar^+)^*/CH_4$[a]	Ar^+/CH_4[b]	$(Kr^+)^*/CH_4$[c]
	$CH(A\,^2\Delta)$	$CH(A\,^2\Delta)$	$CH(A\,^2\Delta)$
$\langle E_v \rangle$	0.13	0.13	0.086
$\langle E_J \rangle$	0.19	0.19	0.23
	$CH(B\,^2\Sigma^-)$	$CH(B\,^2\Sigma^-)$	
$\langle E_v \rangle$	0	0	
$\langle E_J \rangle$	0.23	0.23	

[a] Measured in the Ar afterglow.
[b] Measured in the He afterglow (see the text).
[c] Measured in the Kr afterglow.

$$e^- + CH_2^+ \rightarrow CH(A{:}v' = 0) + H(n = 1) + 3.2 \text{ eV}, \quad (23a)$$

$$e^- + CH_2^+ \rightarrow CH(B{:}v' = 0) + H(n = 1) + 2.9 \text{ eV}, \quad (23b)$$

Assuming that either process (22) or (23) dominates the reaction, the fractions of excess energies deposited into the vibrational and rotational energies of CH(A,B) are estimated to be

$\langle f_v \rangle = 0.057$ and $\langle f_r \rangle = 0.083$ for process (22a),

$\langle f_v \rangle = 0$ and $\langle f_r \rangle = 0.12$ for process (22b),

$\langle f_v \rangle = 0.041$ and $\langle f_r \rangle = 0.059$ for process (23a),

$\langle f_v \rangle = 0$ and $\langle f_r \rangle = 0.079$ for process (23b).

Only 8%–14% of the excess energies is released as the vibrational and rotational energies of CH(A,B), indicating that most of the excess energies is deposited as relative translational energy of fragments. The high $\langle f_t \rangle$ value implies that CH(A,B) are formed through highly repulsive CH_3^{**} and/or CH_2^{**} precursor states in processes (22) and (23).

ACKNOWLEDGMENTS

This work was supported by a Grant-in-Aid for Scientific Research from the Japanese Ministry of Education, Science, and Culture, the Asahi Glass Foundation, and the Ito Science Foundation.

[1] J. F. Prince, C. B. Collins, and W. W. Robertson, J. Chem. Phys. **40**, 2619 (1964).
[2] K. Suzuki and K. Kuchitsu, Chem. Phys. Lett. **56**, 50 (1978).
[3] K. Suzuki, I. Nishiyama, Y. Ozaki, and K. Kuchitsu, Chem. Phys. Lett. **58**, 145 (1978).
[4] I. Nishiyama, Y. Ozaki, K. Suzuki, and K. Kuchitsu, Chem. Phys. Lett. **67**, 258 (1979).
[5] M. Tsuji, H. Obase, M. Matsuo, M. Endoh, and Y. Nishimura, Chem. Phys. **50**, 195 (1980).
[6] M. Tsuji, in *Techniques of Chemistry*, edited by J. M. Farrar and W. H. Saunder, Jr. (Wiley, New York, 1988), Vol. 20, Chap. 9, p. 489.
[7] M. Tsuji, K. Kobarai, S. Yamaguchi, H. Obase, and Y. Nishimura, Chem. Phys. Lett. **166**, 485 (1990).
[8] A. J. Yencha, in *Electron Spectroscopy: Theory, Techniques, and Applications*, edited by C. R. Brundle and A. D. Baker (Academic, New York, 1984), Vol. 5, p. 197.
[9] M. Tsuji, M. Furusawa, and Y. Nishimura, J. Chem. Phys. **92**, 6502 (1990).
[10] M. Tsuji, M. Furusawa, and Y. Nishimura, Chem. Phys. Lett. **166**, 363 (1990).
[11] N. Sadeghi, M. Cheaib, and D. W. Setser, J. Chem. Phys. **90**, 219 (1989).
[12] H. M. Rosenstock, K. Draxl, B. W. Steiner, and J. T. Herron, J. Phys. Chem. Ref. Data **6**, Suppl. No. 1 (1977).
[13] K. P. Huber and G. Herzberg, *Constants of Diatomic Molecules* (Van Nostrand Reinhold, New York, 1979).
[14] M. Tsuji, K. Kobarai, S. Yamaguchi, H. Obase, K. Yamaguchi, and Y. Nishimura, Chem. Phys. Lett. **155**, 481 (1989).
[15] M. Tsuji, K. Kobarai, S. Yamaguchi, and Y. Nishimura, Chem. Phys. Lett. **158**, 470 (1989).
[16] M. Tsuji, K. Kobarai, and Y. Nishimura, J. Chem. Phys. **93**, 3133 (1990).
[17] R. J. Shul, B. L. Upschulte, R. Passarella, R. G. Keesee, and A. W. Castleman, Jr., J. Phys. Chem. **91**, 2556 (1987).
[18] F. C. Fehsenfeld, J. Chem. Phys. **53**, 2000 (1970).
[19] K. Giles, N. G. Adams, and D. Smith, J. Phys. B **22**, 873 (1989).
[20] H. Sekiya, M. Tsuji, and Y. Nishimura, Chem. Phys. Lett. **100**, 494 (1983).
[21] M. Tsuji, J. P. Maier, H. Obase, H. Sekiya, and Y. Nishimura, Chem. Phys. Lett. **137**, 421 (1987).
[22] I. Kovács, *Rotational Structure in the Spectra of Diatomic Molecules* (Hilger, London, 1969).
[23] M. Tsuji, K. Kobarai, H. Obase, H. Kouno, and Y. Nishimura, J. Chem. Phys. (in press).
[24] J. Brzozowski, P. Bunker, N. Elander, and P. Erman, Astrophys. J. **207**, 414 (1976).